

# Enantioselective Synthesis of Sterically Hindered Tertiary $\alpha$ -Aryl Oxindoles via Palladium-Catalyzed Decarboxylative Protonation. An Experimental and Theoretical Mechanistic Investigation

Maria Biosca,<sup>a,§</sup> Mark Jackson,<sup>b,§</sup> Marc Magre,<sup>a,§</sup> Oscar Pàmies,<sup>a,\*</sup> Per-Ola Norrby,<sup>c,\*</sup> Montserrat Diéguez,<sup>a,\*</sup> and Patrick J. Guiry<sup>b,\*</sup>

<sup>a</sup> Universitat Rovira i Virgili, Departament de Química Física i Inorgànica, C/Marcel·lí Domingo, 1, 43007 Tarragona, Spain. E-mails: oscar.pamies@urv.cat and montserrat.dieguez@urv.cat.

<sup>b</sup> Centre for Synthesis and Chemical Biology, School of Chemistry, University College Dublin, Belfield, Dublin 4, Ireland. Email: p.guiry@ucd.ie.

<sup>c</sup> Early Product Development, Pharmaceutical Sciences, IMED Biotech Unit, AstraZeneca, Pepparedsleden 1, SE-431 83 Mölndal, Sweden. Email: Per-Ola.Norrby@astrazeneca.com.

<sup>§</sup> These authors contributed equally to this study.

Received: ((will be filled in by the editorial staff))

 Supporting information for this article is available on the WWW under <http://dx.doi.org/10.1002/adsc.201#####>. ((Please delete if not appropriate))

**Abstract.** We have developed the first catalytic asymmetric preparation of sterically hindered tertiary  $\alpha$ -aryl oxindoles via enantioselective palladium-catalyzed decarboxylative protonation of the corresponding  $\alpha$ -aryl- $\beta$ -amido allyl esters. The reaction occurs under very mild conditions and in short reaction times, providing excellent yields and promising enantioselectivities (ee's up to 78%). We have also performed an experimental

investigation of the reaction mechanism and employed theoretical calculations to understand the nature of the enantioselectivity-determining step.

**Keywords:** Palladium; Enantioselective catalysis; Decarboxylative protonation;  $\alpha$ -Aryl oxindoles; Mechanistic investigations

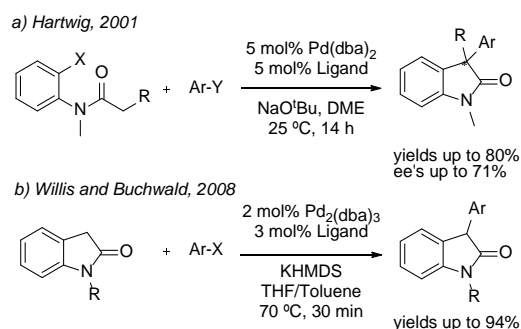
## Introduction

The enantioselective formation of a C-C bond between an aryl group and a carbon  $\alpha$ - to a carbonyl group is one of the most challenging problems in organic chemistry.<sup>[1]</sup> The asymmetric synthesis of  $\alpha$ -aryl carbonyl-containing molecules has attracted much attention over the last decade, due to the presence of this structural motif in a wide range of naturally occurring and biologically active compounds.<sup>[2]</sup>

Oxindoles are endogenous aromatic organic compounds that are found in the tissues and body fluids of mammals. The oxindole skeleton is also present in many natural products which exhibit antiviral, anti-bacterial and anti-carcinogenic properties.<sup>[3]</sup>

The first approach to the asymmetric synthesis of oxindoles was reported by Hartwig (Scheme 1a) in 2001. They reported the preparation of 3,3-disubstituted oxindoles using a Pd-catalyzed intramolecular cyclization with excellent conversions and promising enantioselectivities (ee's up to 71%).<sup>[4]</sup> However, such an approach was not suitable when the substrate had an oxindole core and only quaternary  $\alpha$ -aryl oxindoles were prepared. In contrast to the

catalytic asymmetric synthesis of quaternary  $\alpha$ -aryl carbonyl stereocenters, the synthesis of the corresponding tertiary  $\alpha$ -aryl carbonyl containing compounds remains a challenge due to the ease at which such compounds racemize. As an alternative to the cyclization method, direct metal-catalyzed  $\alpha$ -arylation of carbonyl compounds emerged for a wide range of nucleophiles such as enolates of ketones, esters, nitriles and amides.<sup>[5]</sup>



**Scheme 1.** Previous methodologies for the preparation of  $\alpha$ -aryl oxindoles.

The first metal-catalyzed  $\alpha$ -arylation of oxindoles was reported by Willis<sup>6</sup> and Buchwald's<sup>7</sup> groups independently in 2008 (Scheme 1b). They applied Pd-phosphine complexes to catalyze the  $\alpha$ -arylation of oxindoles with several aryl halides with good to excellent yields. The application of strong bases (such as NaO<sup>t</sup>Bu or KHMDS) is necessary to deprotonate the amidic  $\alpha$ -proton in these approaches to the  $\alpha$ -arylation of oxindoles. However, due to such strong basic media, the asymmetric  $\alpha$ -arylation of oxindoles has not been reported yet because the ease of racemization of the tertiary stereocentre.

An alternative path to the catalytic asymmetric  $\alpha$ -arylation of carbonyls without using strong bases is to perform a Pd-catalyzed decarboxylative protonation of  $\alpha$ -aryl- $\beta$ -keto allyl esters (Scheme 2). With this idea, Guiry has reported the preparation of chiral  $\alpha$ -aryl ketones and isoflavanones via Pd-catalyzed decarboxylative protonation in excellent yields and enantioselectivities with the (*S*)-CF<sub>3</sub>-<sup>t</sup>BuPHOX ligand **1** (Scheme 2a).<sup>8</sup> This methodology was based on the pioneering work of Stoltz who used Pd-decarboxylative protonation of allyl  $\beta$ -ketoesters to prepare  $\alpha$ -alkyl cyclic ketones using the <sup>t</sup>BuPHOX ligand **2**.<sup>9</sup> A relevant finding of Guiry's group was that the electron deficient phosphine-oxazoline ligand (*S*)-CF<sub>3</sub>-<sup>t</sup>BuPHOX **1** provided much higher enantioselectivities than the <sup>t</sup>BuPHOX ligand **2**. The Guiry group has also extensively studied the preparation of sterically hindered  $\alpha$ -allyl- $\alpha$ -aryl carbonyl-containing compounds possessing all-carbon quaternary stereocenters,<sup>10</sup> including oxindoles which required the preparation of a series of  $\alpha$ -aryl- $\beta$ -amido esters **S1-S11**.<sup>11</sup> With these substrates at hand, containing aryl substituents with different electronic and steric properties, we now wish to report the first catalytic asymmetric synthesis of chiral tertiary  $\alpha$ -aryl oxindoles by Pd-catalyzed decarboxylative protonation (Scheme 2b).

Because the use of electron deficient ligands was seen to facilitate the asymmetric Pd-catalyzed decarboxylative protonation of  $\alpha$ -aryl- $\beta$ -keto allyl esters (Scheme 2a),<sup>8a</sup> we focused on electron deficient P,N ligands and applied several  $\pi$ -acceptor phosphite-N ligand families (Figure 1) that Diéguez's group had developed previously. They found that in some asymmetric catalytic transformations the biaryl  $\pi$ -

acceptor phosphite groups in the ligands have a positive effect on activity and widen substrate versatility.<sup>12</sup> The higher flexibility of a biaryl phosphite compared with a phosphine moiety allows these P-N ligands to accommodate a wider range of substrates, thereby yielding excellent enantioselectivities for a broad range of substrates and catalytic reactions.<sup>12</sup> In the present study we applied three phosphite-N ligand families in the Pd-catalyzed decarboxylative protonation of  $\alpha$ -aryl- $\beta$ -amido esters (Figure 1).<sup>13</sup> These phosphite-oxazoline ligands are based on three main ligand structures. The first one is based on the phosphine-oxazoline PHOX ligands **2**, in which the phosphine moiety has been replaced by biaryl phosphite groups (ligands **L1-L4**).<sup>13a-c</sup> In the second one the flat *ortho*-phenylene tether in **L1-L4** has been replaced by an alkyl chain bonded to carbon 4 of the oxazoline moiety (ligands **L5-L8**).<sup>13d-g</sup> In the third one the oxazoline group has been replaced by a more robust pyridine group (ligands **L9-L16**).<sup>13h-i</sup> Several configuration/substituents on the biaryl phosphite moiety have also been studied (**a-e**). Finally, we have also performed an experimental investigation of the reaction mechanism and used theoretical studies primarily to understand the nature of the enantioselectivity-determining step.

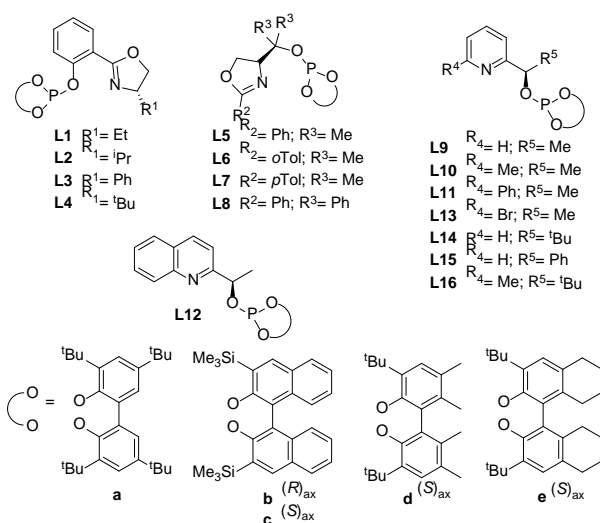
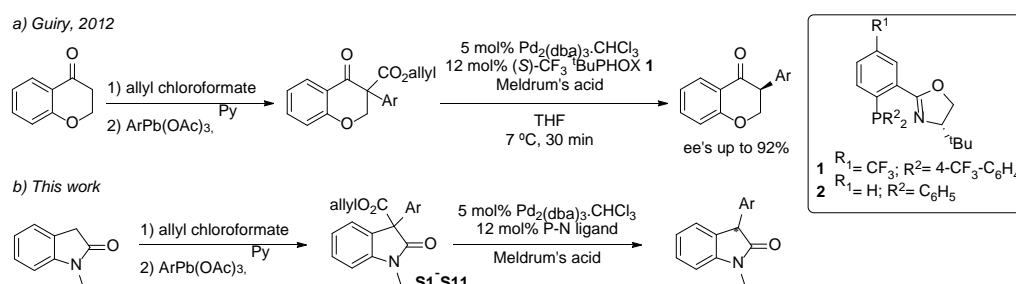


**Figure 1.** Phosphite-nitrogen ligand families.



**Scheme 2.** Enantioselective synthesis of chiral  $\alpha$ -aryl isoflavanones (Scheme 2a) and oxindoles (Scheme 2b) employing Pd-catalyzed decarboxylative protonation.

## Results and Discussion

### Catalytic reactions

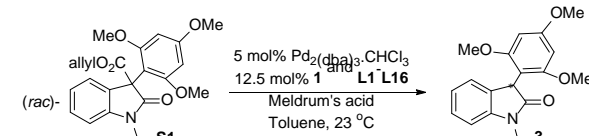
In a first set of experiments we used allyl 1-methyl-2-oxo-3-(2',4',6'-trimethoxyphenyl)indoline-3-carboxylate **S1** as a model substrate using previously developed reaction conditions (Table 1).<sup>[8]</sup> Reactions were therefore performed at room temperature, using 5 mol% of in-situ generated catalyst from Pd<sub>2</sub>(dba)<sub>3</sub>·CHCl<sub>3</sub> and the corresponding ligand in the presence of Meldrum's acid, Table 1. In this protocol catalysts need to be preactivated during 30 min at 40 °C. All catalytic systems were found to give full conversion in less than 2 hours. Disappointingly, the use of the electron deficient phosphine-oxazoline ligand **1** afforded low enantioselectivity (37% ee, Table 1, entry 1).<sup>[14]</sup> The use of related phosphite-oxazoline ligands **L1-L4a**, in which the phosphine moiety in ligand **1** has been replaced by a biaryl phosphite group, provided even lower enantioselectivities (ee's up to 3%, Table 1, entries 2-5). The use of ligands **L5-L8a** provided also lower enantioselectivities than those achieved with ligand **1** (Table 1, entries 6-9). In these cases we found that enantioselectivity is affected by the substituent at the alkyl backbone chain. Thus, the best enantioselectivity (18% ee, entry 9) was achieved with ligand **L8a** which contains phenyl substituents on the alkyl backbone. Similar levels of enantioselectivity were achieved using more robust phosphite-pyridine ligands **L9-L16a** (entry 12, 20% ee). By varying the substituent of the ligand backbone (R<sup>4</sup> and R<sup>5</sup>) with ligands **L9-L16a** we found that the best enantioselectivity was obtained with **L9a** (entry 12), which contain a hydrogen in R<sup>4</sup> and a Me in R<sup>5</sup>.

To improve the enantioselectivities further we used ligands **L8-L9a-e** to study the effect of the biaryl phosphite moiety. The results indicated that enantioselectivity could be increased with the adequate configuration and substituent at the biaryl phosphite moiety (ligand **L9c**, up to 49% ee, entry 14). Thus, ligands **L8-L9c** (entries 11 and 14) with an (*S*)-biaryl phosphite group provided higher enantioselectivities than ligands **L8-L9b** containing an (*R*)-biaryl group (entries 10 and 13). On the other hand, enantioselectivities are very sensitive to variations in the substituents of the biaryl and therefore sensitive to the dihedral angle of the biaryl phosphite group. Accordingly, the use of ligands **L9d-e** (entries 15 and 16), which also contains (*S*)-biaryl phosphite groups, provided lower enantioselectivities than ligand **L9c**.

**Optimization of the reaction conditions.** We next optimized the reaction conditions for ligand **L9c** that had provided the best results, Table 2. The screening of seven solvents (toluene, chloroform, dichloromethane, 1,4-dioxane, tetrahydrofuran, diethyl ether and methyl *tert*-butyl ether (MTBE)) showed that enantioselectivities were higher when

etheral solvents were used (Table 2, entries 1, 4-7 vs 2-3). Of the solvents tested, MTBE had the most positive effect on enantioselectivity (ee's increased to 70%; Table 2, entry 7), albeit with isolated yields up to 64%. This lower yield with MTBE was attributed to the difficulty of a quantitative transfer of the substrate solution to the catalyst mixture due to the low solubility of the substrate in MTBE. To improve yields, both Meldrum's acid and substrate were added as solids to the preactivated solution of the catalyst precursor and ligand. This increased the isolated yields while maintaining the enantioselectivity (entry 11). Another strategy tested, using mixtures of solvents (entries 8-10), was unsuccessful and enantioselectivity decreased, although yields were higher than when using MTBE alone. We also found that catalyst did not need to be preactivated to achieve high yields and ees, although the reaction time required to achieve full conversions increased (entry 12).

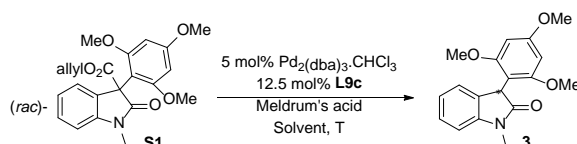
**Table 1.** Initial ligand screening of Pd-catalyzed decarboxylative protonation of **S1**.



Entry <sup>a)</sup>	L	t (min)	Conversion (%) <sup>b)</sup>	ee (%) <sup>c)</sup>
1	<b>1</b>	60	100	37 (+)
2	<b>L1a</b>	60	100	1 (+)
3	<b>L2a</b>	60	100	2 (+)
4	<b>L3a</b>	60	100	1 (+)
5	<b>L4a</b>	60	100	3 (+)
6	<b>L5a</b>	60	100	4 (+)
7	<b>L6a</b>	60	100	3 (+)
8	<b>L7a</b>	60	100	10 (+)
9	<b>L8a</b>	60	100	18 (+)
10	<b>L8b</b>	60	100	11 (+)
11	<b>L8c</b>	60	100	38 (+)
12	<b>L9a</b>	60	100	20 (+)
13	<b>L9b</b>	60	100	9 (+)
14	<b>L9c</b>	120	100	49 (+)
15	<b>L9d</b>	60	100	5 (+)
16	<b>L9e</b>	60	100	4 (+)
17	<b>L10a</b>	120	100	3 (+)
18	<b>L11a</b>	120	100	1 (-)
19	<b>L12a</b>	120	100	2 (-)
20	<b>L13a</b>	120	100	1 (-)
21	<b>L14a</b>	120	100	8 (-)
22	<b>L15a</b>	120	100	17 (-)
23	<b>L16a</b>	120	100	2 (-)

<sup>a)</sup> Reaction conditions: 50 mg substrate (0.125 mmol), 5 mol% Pd<sub>2</sub>(dba)<sub>3</sub>·CHCl<sub>3</sub>, 12.5 mol% Ligand, 2.5 eq. Meldrum's acid. <sup>b)</sup> Determined by <sup>1</sup>H NMR spectroscopy.

<sup>c)</sup> Determined by SFC.

**Table 2.** Reaction optimization: solvent and temperature with ligand **L9c**

Entry <sup>a)</sup>	Solvent	T (°C)	t (h)	% Conversion (% Yield) <sup>b)</sup>	ee (%) <sup>c)</sup>
1	Toluene	23	2	100 (94)	49 (+)
2	CHCl <sub>3</sub>	23	1	<5 (nd)	5 (+)
3	CH <sub>2</sub> Cl <sub>2</sub>	23	1	100 (93)	17 (+)
4	1,4-Dioxane	23	1	100 (93)	54 (+)
5	THF	23	1	100 (94)	46 (+)
6	Et <sub>2</sub> O	23	1	100 (64)	63 (+)
7	MTBE	23	1	100 (60)	70 (+)
8	MTBE:Dioxane (2:1)	23	1	100 (92)	50 (+)
9	MTBE:dioxane (4:1)	23	1	100 (93)	33 (+)
10	MTBE:Toluene (1:1)	23	1	100 (91)	36 (+)
11 <sup>d)</sup>	MTBE	23	1	100 (92)	66 (+)
12 <sup>e)</sup>	MTBE	23	3	100 (93)	70 (+)
13 <sup>e)</sup>	MTBE	5	3	100 (92)	78 (+)
14 <sup>e)</sup>	MTBE	-20	3	43 (nd)	63 (+)
15 <sup>e)</sup>	1,4-Dioxane	40	1	97 (nd)	17 (+)

<sup>a)</sup> Reaction conditions: 50 mg substrate (0.125 mmol), 5 mol% Pd<sub>2</sub>(dba)<sub>3</sub>·CHCl<sub>3</sub>, 12.5 mol% **L9c**, 2.5 eq. Meldrum's acid.

<sup>b)</sup> Determined by <sup>1</sup>H NMR spectroscopy. <sup>c)</sup> Determined by SFC. <sup>d)</sup> Substrate and Meldrum's acid added as solids. <sup>e)</sup> Catalyst precursor, ligand, Meldrum's acid and substrate all together in the Schlenk vessel without catalyst preactivation.

Finally, by decreasing the temperature to 5 °C, enantioselectivity increased up to 78% ee while maintaining the excellent yield (Table 2, entry 13 vs entry 12). Further decreasing the temperature to -20 °C led to a decrease in conversion and enantioselectivity (Table 2, entry 14). We also tested the reaction at 40 °C, since the literature indicated that higher temperatures could provide better enantioselectivities,<sup>[8c]</sup> but the enantioselectivity did not improve (Table 2, entry 15).

**Substrate scope.** After optimizing the reaction, substrates **S2-S11**, with different electronic and steric aryl substituents on the oxindole, were studied. These aryl substituents were chosen due to the facile synthesis of the required aryllead triacetate and the high yields obtained in the arylation of the β-amido allyl esters. In addition, previous results from Guiry had demonstrated the importance of strongly electron-donating substituents in the *ortho*- and *para*-positions for obtaining high enantioselectivities.<sup>[8,9]</sup> The results (Figure 2) underline the importance of bulkiness and of the presence of electron donating substituents for the enantioselectivity.<sup>[15]</sup> The best enantioselectivities (ee's up to 78%) were therefore obtained with the bulkiest and most electronically rich substrates **S1** and

**S2**. When other substrates that had less bulky aryl substituents (**S3** and **S4**) were tested, the enantioselectivity decreased due to the removal of one *ortho*-substituent. Comparing the results for **S3** with those of **S4** we can also determine that substituents at the *meta*-position have almost no effect on the catalytic performance. When the *para*-methoxy group was removed (**S5**), the enantioselectivity decreased but it was higher than those with only one *ortho*-methoxy substituent (**S3** and **S4**). As expected, when non-*ortho*-substituted aryl groups were studied (**S6** and **S7**) almost racemic compounds were obtained.

The importance of an *ortho*-alkoxy substituent was corroborated by its sequential replacement by methyl groups. Products **10** and **11** were obtained with lower ee's than **3** and **7**, respectively. Accordingly, substrates with *ortho*-substituted naphthyl groups (**S10** and **S11**) provided moderate levels of enantioselectivities, comparable to those found when using **S3** and **S4** (ee's up to 28% and 15%, respectively). As a summary, for enantioselectivities to be high, the aryl group of the substrate must contain electron-donating substituents in the *ortho*- and *para*-positions.

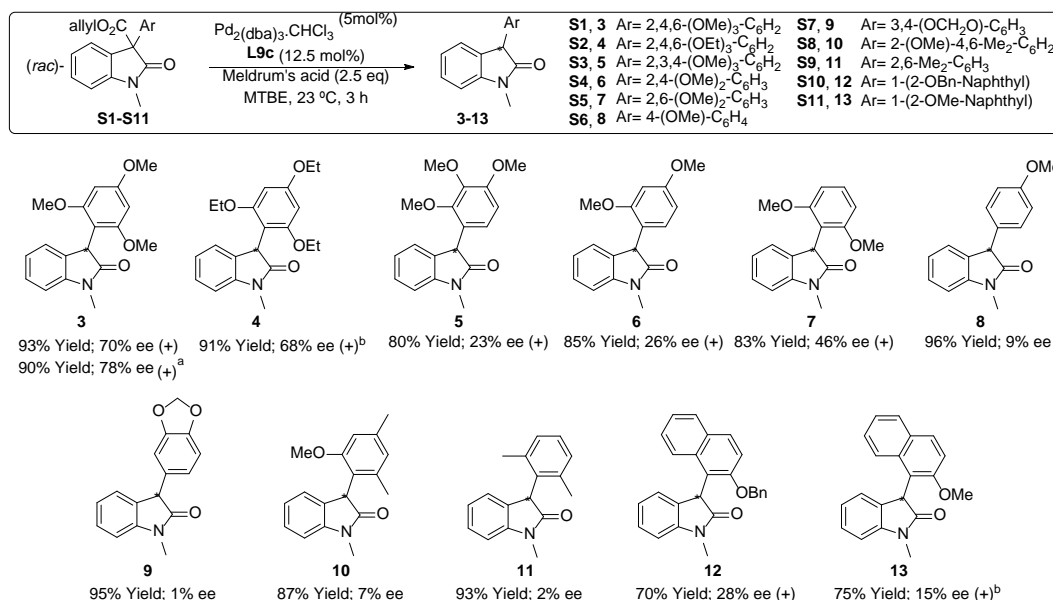
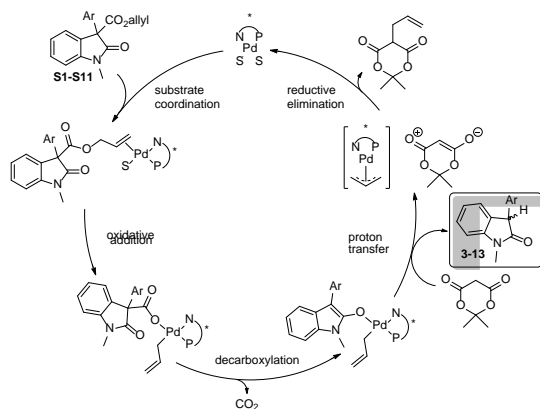


**Figure 2.** Pd-catalyzed decarboxylative protonation of **S1-S11**. Reaction conditions: substrate (0.125 mmol), 5 mol% Pd<sub>2</sub>(dba)<sub>3</sub>·CHCl<sub>3</sub>, 12.5 mol% **L9c**, 2.5 eq. Meldrum's acid. <sup>a</sup> Reaction carried out at 5 °C <sup>b</sup> Reaction carried out in Et<sub>2</sub>O due to insolubility of **S2** and **S11** in MTBE.

#### Study of the key intermediates. Experimental and theoretical studies

Although the mechanism for the asymmetric decarboxylative allylation of allyl β-ketoesters with Pd catalysts has been investigated both experimentally and computationally, the mechanism for decarboxylative protonation is not well understood.<sup>[8d,9c]</sup> The current mechanistic hypothesis for decarboxylative protonation mainly relies on kinetic experiments carried out by Stoltz with allyl β-ketoesters.<sup>[9b,16]</sup> They studied the variation of the substrate concentration over time by NMR spectroscopy and found a zero-order dependence on substrate concentration which indicates that the substrate reacts very fast.<sup>[17]</sup> However, this only gives information about the first two steps of the catalytic cycle, namely the coordination of the substrate and the oxidative addition (Scheme 3).



**Scheme 3.** Proposed catalytic cycle for the enantioselective decarboxylative protonation of allyl β-amido esters.

To obtain a clearer picture of the kinetic profile for the decarboxylative protonation with our allyl β-amido esters, we performed a detailed kinetic study with substrate **S1** using the Pd/**L9c** catalytic system. Initially, we studied the effect of the Pd loading (0.5–2 mM) on activity. It was found that the rate of product formation is proportional to the Pd concentration (Figure 3a). This indicates a first-order dependence and excludes the possibility of polynuclear species as competent catalysts for this transformation. Next, we studied the effect of the substrate concentration on activity. Figure 3b shows that the rate of product formation is independent on the substrate concentration (0.01–0.05 M), which is in agreement with Stoltz's observations. This indicates that the most likely rate determining step is either the decarboxylation or the subsequent proton transfer (Scheme 3). We therefore next studied the effect of the Meldrum's acid concentration on activity. The rate of the decarboxylative protonation of **S1** did not depend on the concentration of Meldrum's acid (0.05–0.2 M; Figure 3c). This zero-order dependence agrees with a rapid protonation step. Further mechanistic insights into the rate determining step of the reaction were obtained by studying the kinetic isotope effect (KIE) of the decarboxylative protonation of **S1** using Meldrum's acid and d<sub>2</sub>-Meldrum's acid (Figure 3d). Reaction monitoring by <sup>1</sup>H-NMR spectroscopy revealed a practically null KIE (KIE ≈ 1.05). This result further confirms that the decarboxylation is the rate determining step.

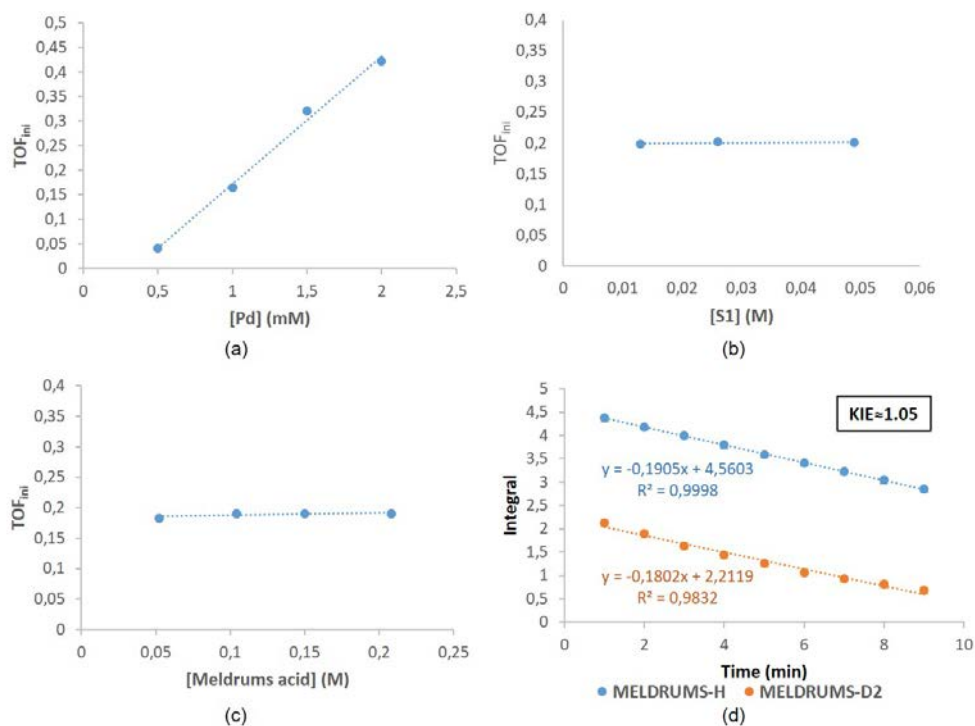
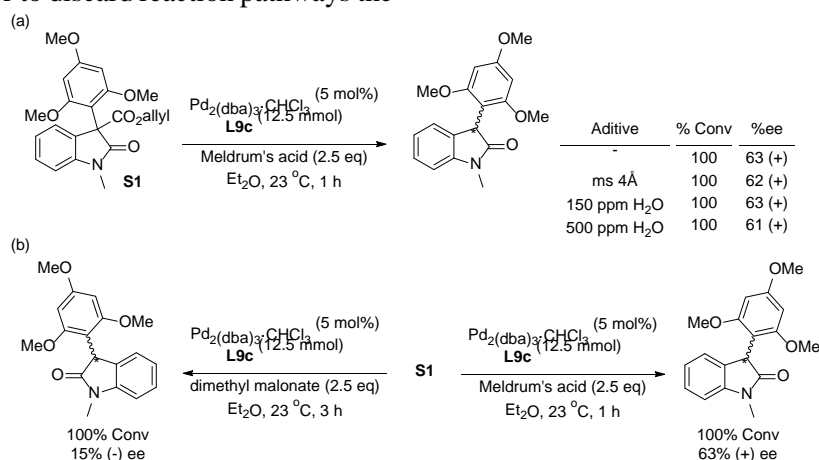


**Figure 3.** Kinetic and kinetic isotope effect measurements of the decarboxylative protonation of **S1** using Pd/**L9c**. (a) Plot of TOF<sub>ini</sub> (measured after 5 min) versus [Pd]. (b) Plot of TOF<sub>ini</sub> (measured after 5 min) versus [S1]. (c) Plot of TOF<sub>ini</sub> (measured after 5 min.) versus Meldrum's acid concentration. (d) Plots of consumption of substrate **S1** using Meldrum's acid and d<sub>2</sub>-Meldrum's acid measured by <sup>1</sup>H NMR spectral integral vs time.

Once the rate determining step had been well established, we moved to study the enantioselectivity-determining step – the proton transfer – by theoretical calculations. However, studying protonation by DFT is complex because there are many reaction pathways that must be considered. These include the direct transfer of the hydrogen from the proton source to the enolate with or without the involvement of water molecules, or a multiple step process in which the proton source protonates the pyridine<sup>[18]</sup> followed by direct transfer of the hydrogen either to the enolate or to the Pd-center (see Figure S1 in the Supporting Information). In order to discard reaction pathways the

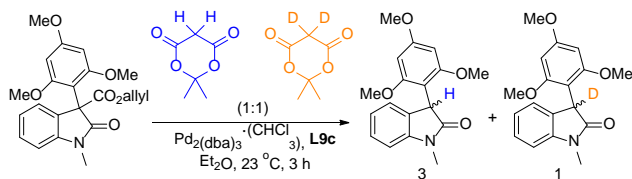
following tests were performed. Firstly, the involvement of water molecules in the transition states (TSs) was studied. We carried out the decarboxylative protonation of **S1** using different amounts of water (including the use of molecular sieves) (Scheme 4a). The same enantioselectivity was obtained in all cases, which allows us to discard the involvement of water in the TSs. We then studied the effect of the proton source on enantioselectivity by replacing Meldrum's acid with dimethyl malonate, leading to a 63% ee (+) using Meldrum's acid and a 15% ee (-) using dimethyl malonate (Scheme 4b).



**Scheme 4.** Decarboxylative protonation of **S1** using (a) different amounts of water and (b) different proton sources.

This experiment indicated that the type of proton source is important in the enantioselectivity determining step and therefore excluded the possibility of a multistep process in which the proton source transfers the proton to the Pd-intermediate prior to the protonation of the enolate. Both experiments agreed with an outer-sphere protonation mechanism in which the Meldrum's acid directly protonates the prochiral enolate formed after the decarboxylation of the allyl  $\beta$ -amido ester (Scheme 3). In preliminary experiments in the asymmetric decarboxylative protonation using the (*S*)-*t*-Bu-PHOX ligand and our model substrate **S1**, we have also investigated a series of other proton sources - cyclopentanone ethyl ester, phenyl sulfonyl acetone, and formic acid, all proton sources originally screened by Stoltz.<sup>[9b]</sup> However, these afforded very low levels of enantioselectivity (6-13% ee). In addition, the employment of acetic acid did not lead to any conversion, highlighting the need, not just for a proton source, but also a reagent that can successfully sequester the allyl unit from palladium. In this case, Meldrum's acid has proven optimal on both counts.

Finally, to study whether the proton transfer is reversible or irreversible, we carried out the decarboxylative protonation of **S1** in a 1:1 mixture of Meldrum's acid and  $d_2$ -Meldrum's acid (Scheme 5). This time a significant KIE was observed ( $KIE \approx 3$ ), indicating that the protonation is irreversible.<sup>[19]</sup>



**Scheme 5.** Competitive decarboxylative protonation of **S1** in the presence of a 1:1 mixture of Meldrum's acid and  $d_2$ -Meldrum's acid.

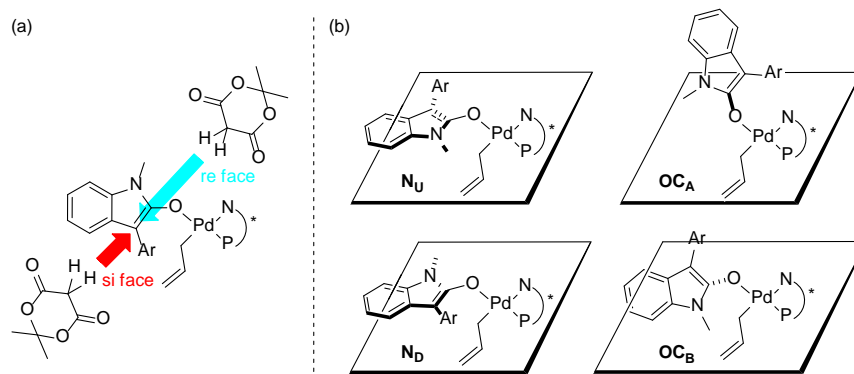
Taking into consideration these conclusions about the nature of the TS a computational study of the TSs arising from the outer-sphere protonation mechanism

was performed in an attempt to explain the enantioselectivity achieved in the Pd-decarboxylative protonation of **S1** using Pd/**L9c**. Only the TSs derived from the Pd-enolates *trans* to the phosphite moiety were calculated (Figure 4a), since it has been shown that  $\sigma$ -allyl complexes with anionic ligands prefer the anion to be *trans* to P than to N.<sup>[20]</sup>

Table 3 shows the calculated energies of all the TSs. These TSs correspond to (a) different relative dispositions of the N-methyl group of the enolate after coordination to Pd (pointing up (**N<sub>U</sub>**) or down (**N<sub>D</sub>**), Figure 4b), (b) different relative dispositions of the oxindole core of the enolate after coordination to Pd (above or below the coordination N-Pd-O-C plane, (**OC<sub>A</sub>** and **OC<sub>B</sub>** in Figure 4b)); and (c) different attack of the Meldrum's acid (through the either *re*- or *si*-faces of the Pd-enolate, Figure 4a).<sup>[21]</sup>

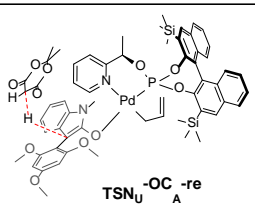
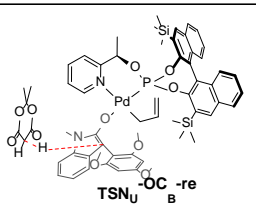
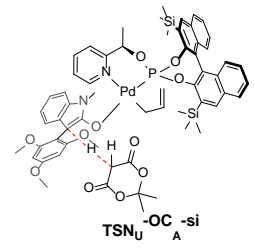
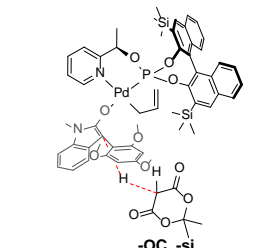
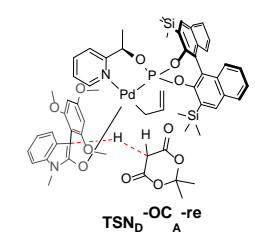
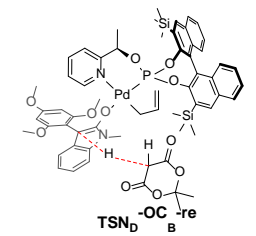
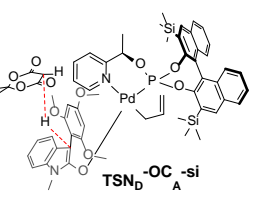
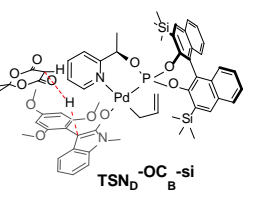
The results (Table 3) show that the two most stable TSs (**TS<sub>N<sub>U</sub>-OC<sub>B</sub>-re</sub>** and **TS<sub>N<sub>U</sub>-OC<sub>B</sub>-si</sub>**) arise from the proton attack on either the enantiotopic *re*-face or the enantiotopic *si*-face of the same Pd-enolate. In this Pd-enolate, the substrate is coordinated in such a way that the N-methyl group is pointing up and the oxazole core is below the coordination plane. The most stable TS, **TS<sub>N<sub>U</sub>-OC<sub>B</sub>-re</sub>**, provides the (*R*)-product.<sup>[22]</sup>

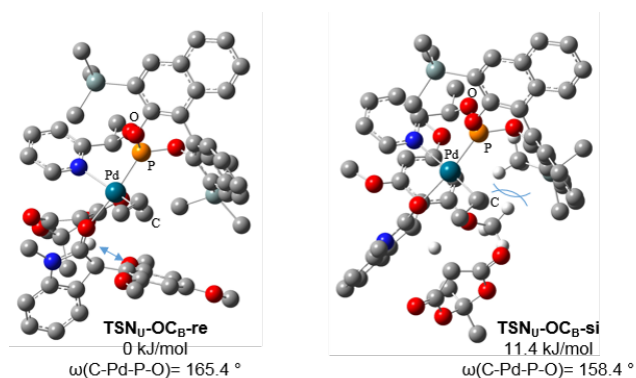
The structure of these two most stable calculated TSs, Figure 5, indicates that the **TS<sub>N<sub>U</sub>-OC<sub>B</sub>-si</sub>** is destabilized due to a steric repulsion between one of the *ortho*-methoxy groups of the substrate and the *ortho*-substituent of the biaryl phosphite moiety. This unfavorable interaction is reflected in a larger dihedral angle  $\omega(C-Pd-P-O)$  in **TS<sub>N<sub>U</sub>-OC<sub>B</sub>-re</sub>** than in **TS<sub>N<sub>U</sub>-OC<sub>B</sub>-si</sub>**. Thus, in **TS<sub>N<sub>U</sub>-OC<sub>B</sub>-si</sub>** the steric interaction pushes the biaryl phosphite moiety away leading to a lower  $\omega$  dihedral angle. In the most stable TS, it is also interesting to note the close proximity of the migrating proton and the oxygen of one of the *ortho*-methoxy groups of the substrate. This suggests that the proton transfer is supported by this *ortho*-methoxy group of the substrate, and explains the lower enantioselectivity achieved when the *ortho*-methoxy groups are replaced by *ortho*-methyls (Figure 2, 70% ee for **3** vs 2% ee for **11**).



**Figure 4.** (a) Representation of the protonation (through either the *re*- and *si*-faces) to the Pd-enolates *trans* to the phosphite moiety. (b) Representation of the different relative dispositions of the enolate took into account in the TSs calculations.

**Table 3.** Calculated energies for the transition states with substrate **S1** using Pd/**L9c**.

Transition state	Energy	Product configuration	Transition state	Energy	Product configuration
 TSN <sub>U</sub> -OC <sub>A</sub> -re	21.8 kJ/mol	R	 TSN <sub>U</sub> -OC <sub>B</sub> -re	0 kJ/mol	R
 TSN <sub>U</sub> -OC <sub>A</sub> -si	53.9 kJ/mol	S	 TSN <sub>U</sub> -OC <sub>B</sub> -si	11.4 kJ/mol	S
 TSN <sub>D</sub> -OC <sub>A</sub> -re	28.0 kJ/mol	R	 TSN <sub>D</sub> -OC <sub>B</sub> -re	30.9 kJ/mol	R
 TSN <sub>D</sub> -OC <sub>A</sub> -si	19.2 kJ/mol	S	 TSN <sub>D</sub> -OC <sub>B</sub> -si	26.5 kJ/mol	S

**Figure 5.** Most stable calculated TSN<sub>U</sub>-OC<sub>B</sub>-re and TSN<sub>U</sub>-OC<sub>B</sub>-si transition states for substrate **S1** and Meldrum's acid using ligand **L9c**. For clarity, only the hydrogens involved in the protonation are shown. For the TSN<sub>U</sub>-OC<sub>B</sub>-si, the hydrogens involved in the steric interaction are also shown. Relative free energies in solution and in kJ/mol respect to the corresponding lowest energy transition state.

The analysis of all calculated DFT structures can be reflected in a quadrant diagram that explains the stereoselectivity. In this quadrant model, the pyridine group of the ligand blocks the upper left quadrant and

one of the aryls of the biaryl phosphite group partly occupies the lower right quadrant making it semi-hindered (Figure 6a). Also, the allyl ligand occupies the upper right quadrant (Figure 6a). In this way, the ligand and the allyl group impose a very sterically hindered chiral environment so that, in the most stable TSS, the oxindole core occupies the free lower left quadrant and only the aryl group slightly occupies the semihindered lower right quadrant (Figure 6b). However, for the less stable TSS, in which the oxindole core is placed above the coordination plane (TSsN<sub>x</sub>-OC<sub>A</sub>), the oxindole core is forced to partially occupy the upper quadrants (Figure 6c), which causes its destabilization. This quadrant model also helps to rationalize the lack of enantiocontrol found with ligands **L9d** and **L9e** (Table 1, entries 15 and 16). These ligands contain less bulky *ortho*-substituents in the biaryl phosphite moiety than **L9c**, which results in a lower occupancy of the semi-hindered lower right quadrant. Therefore, the above mentioned steric interaction between one of the *ortho*-methoxy substituents of the substrate and the substituent of the biaryl phosphite moiety diminishes considerably and therefore the two TSs leading to opposite product enantiomers have a more similar energy.

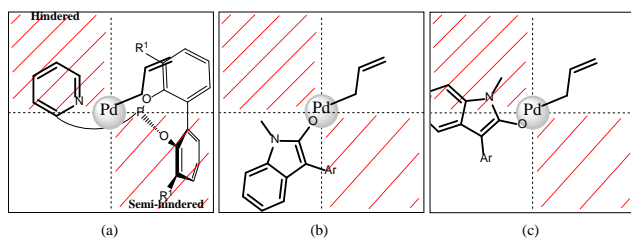


**Figure 6.** Quadrant diagram describing the enantioselective substrate-ligand interactions.

Finally, to study how the *ortho*-substitution of the aryl moiety of the substrate affected enantioselectivity, we ran analogous calculations for substrates **S4** and **S6**. The results, which can be found in the Supporting Information, indicate that again the most stable TSs for both substrates are the **TSN<sub>U</sub>-OC<sub>B</sub>-re** and **TSN<sub>U</sub>-OC<sub>B</sub>-si** (Figure 7). The results also indicate that due to the lack of one or both *ortho*-substituents, the energy difference between the two most stable TSs is smaller than for the two most stable TSs for substrate **S1** ( $\Delta\Delta G_{\text{calc}} \approx 1.5$  kJ/mol for **S4** and **S6** vs  $\Delta\Delta G_{\text{calc}} \approx 11.4$  kJ/mol for **S1**). This can be attributed to two main reasons. Firstly, the above mentioned steric hindrance between the *ortho*-substituent and the biaryl phosphite moiety is less important and therefore the dihedral angle  $\omega$  for the TSs, leading to opposite enantiomers for each substrate, are very similar. Secondly, the presence of two *ortho*-methoxy groups is needed to ensure that one methoxy group is in a good position to stabilize the proton and support its migration.

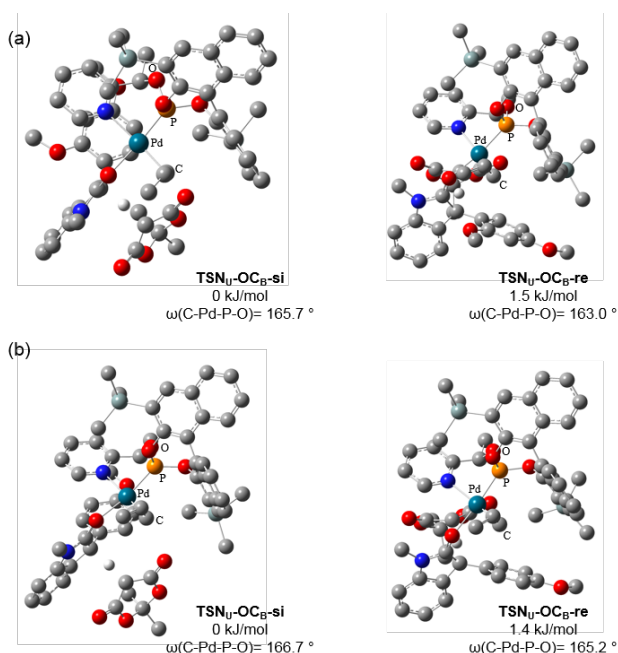


**Figure 7.** Most stable calculated **TSN<sub>U</sub>-OC<sub>B</sub>-re** and **TSN<sub>U</sub>-OC<sub>B</sub>-si** transition states for substrates (a) **S4** and (b) **S6** with Meldrum's acid using ligand **L9c**. All hydrogen atoms have been omitted for clarity except those involved in the protonation. Relative free energies in solution and in kJ/mol respect to the corresponding lowest energy transition state.

## Conclusion

We have developed the first catalytic asymmetric synthesis of tertiary sterically hindered  $\alpha$ -aryl oxindoles via enantioselective Pd-catalyzed decarboxylative protonation of the corresponding  $\alpha$ -aryl- $\beta$ -amido allyl esters. The method utilizes readily accessible  $\alpha$ -aryl- $\beta$ -amido allyl esters and commercially available Meldrum's acid as the proton donor. The reaction occurs under very mild conditions and in short reaction times, providing excellent yields and promising enantioselectivities (ee's up to 78%). After the screening of three large series of phosphite-N (N=oxazoline and pyridine) ligand families we found that the best results were obtained with a readily accessible phosphite-pyridine ligand library. The introduction of an enantiopure (*S*)-biaryl phosphite moiety with bulky substituents in the *ortho*-positions played an essential role in increasing the enantioselectivity of the Pd-catalytic systems. For enantioselectivities to be high, the aryl group of the substrate must contain strongly electron-donating substituents in the *ortho*- and *para*-positions. In this study we have been therefore able to identify a readily accessible phosphite-pyridine palladium catalytic system (Pd/**L9c**) that can be used for the preparation of hindered and electron rich  $\alpha$ -aryl oxindoles with excellent yields (up to 96%) and promising enantioselectivities (ee's up to 78%). Kinetic studies in a practical regime and KIE experiments indicated that decarboxylation is the rate determining step. The combination of an experimental investigation and theoretical studies were used to understand the nature of the selective-determining step – the proton transfer. The enantioselectivity and the effect of the ligand parameters could be rationalized in terms of a simple quadrant model.

## Experimental Section

### General Considerations

All reactions were performed under an inert atmosphere of nitrogen in flame-dried glassware with magnetic stirring. All reagents were obtained from commercial sources and used without further purification unless otherwise stated. Anhydrous methyl *tert*-butyl ether (MTBE) was dried refluxing it over sodium and benzophenone. All other solvents were obtained from dry solvent dispenser. Aryl lead triacetates ( $\text{ArPb}(\text{OAc})_3$ ) were synthesized according to literature procedures.<sup>[8a]</sup>  $\alpha$ -Aryl- $\beta$ -amido allyl esters **S1** and **S3-S11** have been synthesized and characterized following a reported procedure.<sup>[11]</sup>  $\text{Pd}_2\text{dba}_3 \cdot \text{CHCl}_3$  was freshly synthesized following reported method.<sup>[23]</sup> Meldrum's acid was recrystallized from ethyl acetate before its use. Ligands **1**,<sup>[8a]</sup> **L1-L4**,<sup>[13a]</sup> **L5-L8**,<sup>[13d]</sup> **L9-L16**<sup>[13h]</sup> and  $d_2$ -Meldrum's acid<sup>[24]</sup> were prepared as previously described. Hydroxyl-pyridine intermediate for the preparation of ligands **L9e** was prepared following the reported procedure.<sup>[13h]</sup> Phosphorochloridite was easily prepared in one step from the corresponding binaphthol.<sup>[25]</sup> Thin layer chromatography (TLC) was performed on aluminum plates precoated with silica gel F254. They were visualized with UV-light (254 nm) fluorescence quenching, or by charring with acidic vanillin solution (vanillin,  $\text{H}_2\text{SO}_4$  in ethanol).  $[\alpha]_{\text{D}}^{20}$  values have been determined using PE MC240 apparatus with a sodium (Na) lamp at 589 nm.  $^1\text{H}$ ,  $^{13}\text{C}\{^1\text{H}\}$ ,

and  $^{31}\text{P}\{^1\text{H}\}$  NMR spectra were recorded using a 400 MHz spectrometer. Chemical shifts are relative to that of  $\text{SiMe}_4$  ( $^1\text{H}$  and  $^{13}\text{C}$ ) as internal standard or  $\text{H}_3\text{PO}_4$  ( $^{31}\text{P}$ ) as external standard.  $^1\text{H}$ ,  $^{13}\text{C}$  and  $^{31}\text{P}$  spectral assignments were made on the basis of  $^1\text{H}$ - $^1\text{H}$  gCOSY,  $^1\text{H}$ - $^{13}\text{C}$  gHSQC and  $^1\text{H}$ - $^{31}\text{P}$  gHMBC experiments.

### Preparation of phosphite-pyridine ligand L9e

The corresponding phosphorochloridite (1.1 mmol) produced *in situ* was dissolved in toluene (5 mL) and pyridine (0.19 mL, 2.3 mmol) was added. The corresponding hydroxyl-pyridine compound (1 mmol) was dried azeotropically with toluene (3 x 2 mL) and then dissolved in toluene (5 mL) to which pyridine (0.19 mL, 2.3 mmol) was added. The phosphorochloridite solution was transferred slowly at room temperature to the solution of hydroxyl-pyridine. Reaction was left at 80 °C for 90 min. Pyridine salts were removed through filtration. Evaporation of the solvent gave white foam, which was purified by using flash chromatography under argon in dry alumina (Toluene:Hexane:  $\text{NEt}_3$ , 5:5:0.1) to produce the corresponding ligand as a white solid. Yield: 345.9 mg (56%);  $^{31}\text{P}$  NMR ( $\text{C}_6\text{D}_6$ ):  $\delta$  = 136.8 ppm (s);  $^1\text{H}$  NMR ( $\text{C}_6\text{D}_6$ ):  $\delta$  = 1.1-1.3 (m, 6H,  $\text{CH}_2$ ), 1.38 (s, 9H,  $\text{CH}_3$ ,  $^t\text{Bu}$ ), 1.45 (d, 3H,  $\text{CH}_3$ ,  $^3J_{\text{H-H}} = 6.7$  Hz), 1.57 (s, 9H,  $\text{CH}_3$ ,  $^t\text{Bu}$ ), 2.1-2.6 (m, 10H,  $\text{CH}_2$ ), 5.35 (m, 1H,  $\text{CH-O}$ ), 6.54 (m, 1H,  $\text{CH=}$ ), 6.9-7.21 (m, 4H,  $\text{CH=}$ ), 8.3 (m, 1H,  $\text{CH=}$ ).  $^{13}\text{C}$  NMR ( $\text{C}_6\text{D}_6$ ):  $\delta$  = 22.7 ( $\text{CH}_2$ ), 22.9 ( $\text{CH}_2$ ), 23.1 ( $\text{CH}_2$ ), 23.2 ( $\text{CH}_2$ ), 23.6 ( $\text{CH}_3$ ), 27.2 ( $\text{CH}_2$ ), 27.5 ( $\text{CH}_2$ ), 29.5 ( $\text{CH}_2$ ), 29.6 ( $\text{CH}_2$ ), 30.8 ( $\text{CH}_3$ ,  $^t\text{Bu}$ ), 31.0 ( $\text{CH}_3$ ,  $^t\text{Bu}$ ), 34.3 (C,  $^t\text{Bu}$ ), 34.6 (C,  $^t\text{Bu}$ ), 75.7 (d,  $\text{CH-O}$ ,  $^2J_{\text{C-P}} = 9.3$  Hz), 119.7 ( $\text{CH=}$ ), 121.7 ( $\text{CH=}$ ), 125.3 (C), 128.9 ( $\text{CH=}$ ), 130.1 (C), 130.9 (C), 132.3 (C), 132.9 (C), 134.8 (C), 135.1 (C), 135.8 ( $\text{CH=}$ ), 137.8 (C), 138.3 (C), 145.0 (C), 145.4 (C), 148.6 ( $\text{CH=}$ ), 162.9 (C). MS HR-ESI [found 557.3062,  $\text{C}_{35}\text{H}_{44}\text{NO}_3\text{P}$  ( $\text{M}^+$ ) requires 557.3059].

### General procedure for enantioenriched protonated compounds (3-13)

$\text{Pd}_2(\text{dba})_3\cdot\text{CHCl}_3$  (0.0125 mmol, 6.6 mg), phosphite-pyridine **L9c** (0.016 mmol, 9 mg), substrate (0.125 mmol), Meldrum's acid (2.5 eq, 0.31 mmol, 42.4 mg) were added to a flame dried Schlenk flask and dry methyl *tert*-butyl ether (MTBE) (for **S1**, **S3-S10**) or diethyl ether (for **S2** and **S11**) (5 ml) were added. The suspension was stirred at room temperature for 3 h. The solvent was removed under vacuum and the resulting residue was purified by silica gel column chromatography (pentane: EtOAc), to achieve the corresponding product.

**1-Methyl-3-(2',4',6'-trimethoxyphenyl)indolin-2-one 3:** Yield: 36.4 mg (93%) as a yellowish solid ( $[\alpha]_{\text{D}}^{20}$ : +24.4° (*c* 0.82 in  $\text{CH}_2\text{Cl}_2$ ) for 70% ee);  $^1\text{H}$  NMR ( $\text{CDCl}_3$ ):  $\delta$  = 3.32 (s, 3H,  $\text{NCH}_3$ ), 3.41 (s, 3H,  $\text{OCH}_3$ ), 3.76 (s, 3H,  $\text{OCH}_3$ ), 3.87 (s, 3H,  $\text{OCH}_3$ ), 5.08 (s, 1H,  $\text{CH}$ ), 6.03 (d,  $^4J_{\text{H-H}} = 2.6$  Hz, 1H,  $\text{CH=}$ ), 6.21 (d,  $^4J_{\text{H-H}} = 2.6$  Hz, 1H,  $\text{CH=}$ ), 6.81 (d,  $^3J_{\text{H-H}} = 10.5$  Hz, 1H,  $\text{CH=}$ ), 6.95 (m, 2H,  $\text{CH=}$ ), 7.22 (t,  $^3J_{\text{H-H}} = 10.6$  Hz, 1H,  $\text{CH=}$ ).  $^{13}\text{C}$  NMR ( $\text{CDCl}_3$ ):  $\delta$  = 26.1 ( $\text{CH}_3$ ,  $\text{NCH}_3$ ), 42.0 (CH), 55.2 ( $\text{CH}_3$ ,  $\text{OCH}_3$ ), 56.1 ( $\text{CH}_3$ ,  $\text{OCH}_3$ ), 91.1 ( $\text{CH=}$ ), 92.0 ( $\text{CH=}$ ), 106.8 (C), 107.1 ( $\text{CH=}$ ), 122.0 ( $\text{CH=}$ ), 123.1 ( $\text{CH=}$ ), 127.1 ( $\text{CH=}$ ), 130.2 (C), 144.2 (C), 158.3 (C), 159.1 (C), 160.3 (C), 178.0 (C=O). TOF-HRMS (ESI+): *m/z* = 314.1389, calcd. for  $\text{C}_{18}\text{H}_{20}\text{NO}_4$  [ $\text{M}+\text{H}$ ] $^+$ : 314.1392. ee determined by SFC using Chiralcel IC-3 column (flow: 3 ml/min, 70:30  $\text{scCO}_2$ :MeOH;  $\lambda$  = 254.0 nm).  $R_T$  (+): 1.71 min (major),  $R_T$  (-): 2.29 min (minor).

**1-Methyl-3-(2',4',6'-triethoxyphenyl)indolin-2-one 4:** Yield: 40.4 mg (91%) as a white solid ( $[\alpha]_{\text{D}}^{20}$ : +30.0° (*c* 0.98 in  $\text{CH}_2\text{Cl}_2$ ) for 68% ee);  $^1\text{H}$  NMR ( $\text{CDCl}_3$ ):  $\delta$  = 0.89 (t, 3H,  $\text{CH}_3$ ,  $\text{OEt}$ ,  $^3J_{\text{H-H}} = 6.8$  Hz), 1.38 (t, 3H,  $\text{CH}_3$ ,  $\text{OEt}$ ,  $^3J_{\text{H-H}} = 7.2$  Hz), 1.41 (t, 3H,  $\text{CH}_3$ ,  $\text{OEt}$ ,  $^3J_{\text{H-H}} = 7.2$  Hz), 3.26 (s, 3H,  $\text{NCH}_3$ ), 3.56 (m, 1H,  $\text{CH}_2$ ,  $\text{OEt}$ ), 3.78 (m, 1H,  $\text{CH}_2$ ,  $\text{OEt}$ ), 3.99 (m, 2H,  $\text{CH}_2$ ,  $\text{OEt}$ ), 4.11 (m, 2H,  $\text{CH}_2$ ,  $\text{OEt}$ ), 5.12 (s, 1H,  $\text{CH}$ ), 5.97 (d, 1H,  $\text{CH=}$ ,  $^4J_{\text{H-H}} = 2.0$  Hz), 6.18 (d, 1H,

$\text{CH=}$ ,  $^4J_{\text{H-H}} = 2.4$  Hz), 6.80 (d, 1H,  $\text{CH=}$ ,  $^3J_{\text{H-H}} = 7.2$  Hz), 6.95 (m, 2H,  $\text{CH=}$ ), 7.22 (m, 1H,  $\text{CH=}$ ).  $^{13}\text{C}$  NMR ( $\text{CDCl}_3$ ):  $\delta$  = 14.2 ( $\text{CH}_3$ ,  $\text{OEt}$ ), 14.8 ( $\text{CH}_3$ ,  $\text{OEt}$ ), 14.9 ( $\text{CH}_3$ ,  $\text{OEt}$ ), 26.2 ( $\text{CH}_3$ ,  $\text{NCH}_3$ ), 42.1 (CH), 63.4 ( $\text{CH}_2$ ,  $\text{OEt}$ ), 64.2 ( $\text{CH}_2$ ,  $\text{OEt}$ ), 92.0 ( $\text{CH=}$ ), 92.2 ( $\text{CH=}$ ), 107.0 ( $\text{CH=}$ ), 121.8 (C), 123.2 ( $\text{CH=}$ ), 127.0 ( $\text{CH=}$ ), 130.5 (C), 144.6 (C), 158.0 (C), 158.7 (C), 159.9 (C), 178.0 (C=O). TOF-HRMS (ESI+): *m/z* = 356.1862, calcd. for  $\text{C}_{21}\text{H}_{26}\text{NO}_4$  [ $\text{M}+\text{H}$ ] $^+$ : 356.1860. ee determined by SFC using Chiralpak IA column (flow: 3 ml/min, 90:10  $\text{scCO}_2$ :MeOH;  $\lambda$  = 254.0 nm).  $R_T$  (-): 1.55 min (minor),  $R_T$  (+): 2.42 min (major).

**1-Methyl-3-(2',3',4'-trimethoxyphenyl)indolin-2-one 5:** Yield: 31.3 mg (80%) as a white solid ( $[\alpha]_{\text{D}}^{20}$ : +3.5° (*c* 0.77 in  $\text{CH}_2\text{Cl}_2$ ) for 23% ee);  $^1\text{H}$  NMR ( $\text{CDCl}_3$ ):  $\delta$  = 3.28 (s, 3H,  $\text{NCH}_3$ ), 3.62 (s, 3H,  $\text{OCH}_3$ ), 3.82 (s, 3H,  $\text{OCH}_3$ ), 3.84 (s, 3H,  $\text{OCH}_3$ ), 4.62 (s, 1H,  $\text{CH}$ ), 6.62 (d,  $^3J_{\text{H-H}} = 6.4$  Hz, 1H,  $\text{CH=}$ ), 6.81 (d,  $^3J_{\text{H-H}} = 6.8$  Hz, 1H,  $\text{CH=}$ ), 6.88 (d,  $^3J_{\text{H-H}} = 6.5$  Hz, 1H,  $\text{CH=}$ ), 7.00 (m, 2H,  $\text{CH=}$ ), 7.24 (m, 1H,  $\text{CH=}$ ).  $^{13}\text{C}$  NMR ( $\text{CDCl}_3$ ):  $\delta$  = 26.1 ( $\text{CH}_3$ ,  $\text{NCH}_3$ ), 48.0 (CH), 56.1 ( $\text{CH}_3$ ,  $\text{OCH}_3$ ), 60.2 ( $\text{CH}_3$ ,  $\text{OCH}_3$ ), 107.4 ( $\text{CH=}$ ), 107.9 ( $\text{CH=}$ ), 122.4 ( $\text{CH=}$ ), 124.0 (C), 124.2 ( $\text{CH=}$ ), 124.4 ( $\text{CH=}$ ), 128.0 ( $\text{CH=}$ ), 130.1 (C), 142.1 (C), 144.2 (C), 152.3 (C), 153.9 (C), 176.2 (C=O). TOF-HRMS (ESI+): *m/z* = 314.1387, calcd. for  $\text{C}_{18}\text{H}_{20}\text{NO}_4$  [ $\text{M}+\text{H}$ ] $^+$ : 314.1392. ee determined by SFC using Chiralcel IC-3 column (flow: 3 ml/min, 70:30  $\text{scCO}_2$ :MeOH;  $\lambda$  = 254.0 nm).  $R_T$  (+): 2.77 min (major),  $R_T$  (-): 5.85 min (minor).

**3-(2',4'-Dimethoxyphenyl)-1-methylindolin-2-one 6:** Yield: 33.3 mg (85%) as a yellowish solid ( $[\alpha]_{\text{D}}^{20}$ : +2.40° (*c* 0.75 in  $\text{CH}_2\text{Cl}_2$ ) for 26% ee);  $^1\text{H}$  NMR ( $\text{CDCl}_3$ ):  $\delta$  = 3.27 (s, 3H,  $\text{NCH}_3$ ), 3.43 (s,  $\text{CH}_3$ ,  $\text{OCH}_3$ ), 3.89 (s, 3H,  $\text{OCH}_3$ ), 5.18 (s, 1H,  $\text{CH}$ ), 6.42 (d,  $^3J_{\text{H-H}} = 6.8$  Hz, 1H,  $\text{CH=}$ ), 6.62 (d,  $^3J_{\text{H-H}} = 6.8$  Hz, 1H,  $\text{CH=}$ ), 6.81 (d,  $^3J_{\text{H-H}} = 6.8$  Hz, 1H,  $\text{CH=}$ ), 6.93 (m, 2H,  $\text{CH=}$ ), 7.20 (m, 2H,  $\text{CH=}$ ).  $^{13}\text{C}$  NMR ( $\text{CDCl}_3$ ):  $\delta$  = 26.0 ( $\text{CH}_3$ ,  $\text{NCH}_3$ ), 42.1 (CH), 55.8 ( $\text{CH}_3$ ,  $\text{OCH}_3$ ), 55.9 ( $\text{CH}_3$ ,  $\text{OCH}_3$ ), 104.0 ( $\text{CH=}$ ), 105.1 ( $\text{CH=}$ ), 107.1 ( $\text{CH=}$ ), 114.1 (C), 121.8 ( $\text{CH=}$ ), 123.2 ( $\text{CH=}$ ), 127.2 ( $\text{CH=}$ ), 128.8 ( $\text{CH=}$ ), 129.8 (C), 144.2 (C), 158.0 (C), 158.5 (C), 177.8 (C=O). TOF-HRMS (ESI+): *m/z* = 284.1282, calcd. for  $\text{C}_{17}\text{H}_{18}\text{NO}_3$  [ $\text{M}+\text{H}$ ] $^+$ : 284.1287. ee determined by SFC using Chiralcel IC-3 column (flow: 3 ml/min, 90:10  $\text{scCO}_2$ :MeOH;  $\lambda$  = 254.0 nm).  $R_T$  (+): 7.43 min (major),  $R_T$  (-): 8.19 min (minor).

**3-(2',6'-Dimethoxyphenyl)-1-methylindolin-2-one 7:** Yield: 29.4 mg (83%) as a white solid ( $[\alpha]_{\text{D}}^{20}$ : +14.6° (*c* = 0.28 in  $\text{CH}_2\text{Cl}_2$ ) for 46% ee);  $^1\text{H}$  NMR ( $\text{CDCl}_3$ ):  $\delta$  = 3.28 (s, 3H,  $\text{NCH}_3$ ), 3.70 (s, 3H,  $\text{OCH}_3$ ), 3.78 (s, 3H,  $\text{OCH}_3$ ), 4.80 (s, 1H,  $\text{CH}$ ), 6.48 (m, 2H,  $\text{CH=}$ ), 6.83 (d,  $^3J_{\text{H-H}} = 6.8$  Hz, 1H,  $\text{CH=}$ ), 6.98 (m, 2H,  $\text{CH=}$ ), 7.06 (m, 1H,  $\text{CH=}$ ), 7.25 (m, 1H,  $\text{CH=}$ ).  $^{13}\text{C}$  NMR ( $\text{CDCl}_3$ ):  $\delta$  = 26.1 ( $\text{CH}_3$ ,  $\text{NCH}_3$ ), 47.2 (CH), 55.6 ( $\text{CH}_3$ ,  $\text{OCH}_3$ ), 55.8 ( $\text{CH}_3$ ,  $\text{OCH}_3$ ), 99.1 ( $\text{CH=}$ ), 104.1 ( $\text{CH=}$ ), 107.6 ( $\text{CH=}$ ), 118.0 (C), 122.1 ( $\text{CH=}$ ), 124.0 ( $\text{CH=}$ ), 127.9 ( $\text{CH=}$ ), 129.9 ( $\text{CH=}$ ), 130.1 (C), 144.0 (C), 158.1 (C), 160.5 (C), 176.8 (C=O). TOF-HRMS (ESI+): *m/z* = 284.1280, calcd. for  $\text{C}_{17}\text{H}_{18}\text{NO}_3$  [ $\text{M}+\text{H}$ ] $^+$ : 284.1287. ee determined by SFC using Chiralcel IC-3 column (flow: 3 ml/min, 90:10  $\text{scCO}_2$ :MeOH;  $\lambda$  = 254.0 nm).  $R_T$  (+): 6.75 min (major),  $R_T$  (-): 7.52 min (minor).

**3-(4'-Methoxyphenyl)-1-methylindolin-2-one 8:** Yield: 30.4 mg (96%) as a white solid (9% ee);  $^1\text{H}$  NMR ( $\text{CDCl}_3$ ):  $\delta$  = 3.24 (s, 3H,  $\text{NCH}_3$ ), 3.78 (s, 3H,  $\text{OCH}_3$ ), 4.57 (s, 1H,  $\text{CH}$ ), 6.87 (m, 3H,  $\text{CH=}$ ), 7.06 (m, 1H,  $\text{CH=}$ ), 7.15 (m, 3H,  $\text{CH=}$ ), 7.33 (m, 1H,  $\text{CH=}$ ).  $^{13}\text{C}$  NMR ( $\text{CDCl}_3$ ):  $\delta$  = 26.1 ( $\text{CH}_3$ ,  $\text{NCH}_3$ ), 51.1 (CH), 55.2 ( $\text{CH}_3$ ,  $\text{OCH}_3$ ), 108.0 ( $\text{CH=}$ ), 114.2 ( $\text{CH=}$ ), 122.5 ( $\text{CH=}$ ), 124.8 ( $\text{CH=}$ ), 128.0 ( $\text{CH=}$ ), 128.2 (C), 129.0 (C), 129.5 ( $\text{CH=}$ ), 144.2 (C), 159.0 (C), 176.0 (C=O). TOF-HRMS (ESI+): *m/z* = 254.1181, calcd. for  $\text{C}_{16}\text{H}_{17}\text{NO}_2$  [ $\text{M}+\text{H}$ ] $^+$ : 254.1173. ee determined by SFC using Chiralcel IC-3 column (flow: 3 ml/min, 70:30  $\text{scCO}_2$ :MeOH;  $\lambda$  = 254.0 nm).  $R_T$  (major): 1.79 min,  $R_T$  (minor): 2.04 min.

**3-(Benzo[d][1,3]dioxol-5-yl)-1-methylindolin-2-one 9:** Yield: 31.7 mg (95%) as a yellowish solid (1% ee);  $^1\text{H}$  NMR ( $\text{CDCl}_3$ ):  $\delta$  = 3.26 (s, 3H,  $\text{NCH}_3$ ), 4.51 (s, 1H,  $\text{CH}$ ), 5.91 (s,

2H, CH<sub>2</sub>), 6.60 (s, 1H, CH=), 6.69 (m, 1H, CH=), 6.76 (m, 1H, CH=), 6.87 (d, <sup>3</sup>J<sub>H-H</sub> = 6.4 Hz, 1H, CH=), 7.08 (t, <sup>3</sup>J<sub>H-H</sub> = 6.5 Hz, 1H, CH=), 7.18 (d, <sup>3</sup>J<sub>H-H</sub> = 6.6 Hz, 1H, CH=), 7.35 (t, <sup>3</sup>J<sub>H-H</sub> = 6.7 Hz, 1H, CH=). <sup>13</sup>C NMR (CDCl<sub>3</sub>): δ = 26.1 (CH<sub>3</sub>, NCH<sub>3</sub>), 51.5 (CH), 101.2 (CH<sub>2</sub>), 108.0 (CH=), 108.2 (CH=), 122.0 (CH=), 122.8 (CH=), 124.8 (CH=), 128.3 (CH=), 128.5 (C), 130.0 (C), 144.2 (C), 147.1 (C), 148.0 (C), 176.0 (C=O). TOF-HRMS (ESI+): m/z = 268.0967, calcd. for C<sub>16</sub>H<sub>14</sub>NO<sub>3</sub> [M+H]<sup>+</sup>: 268.0974. ee determined by SFC using Chiralcel IC-3 column (flow: 3 ml/min, 70:30 scCO<sub>2</sub>:MeOH; λ = 254.0 nm). R<sub>T</sub> (major): 1.88 min, R<sub>T</sub> (minor): 2.07 min.

**3-(2'-Methoxy-4',6'-dimethylphenyl)-1-methylindolin-2-one 10:** Yield: 30.6 mg (87%) as a white solid (7% ee); <sup>1</sup>H NMR (CDCl<sub>3</sub>): δ = 1.62 (s, 3H, CH<sub>3</sub>), 2.49 (s, 3H, CH<sub>3</sub>), 3.31 (s, 3H, NCH<sub>3</sub>), 3.68 (s, 3H, OCH<sub>3</sub>), 4.67 (s, 1H, CH), 6.41 (s, 1H, CH=), 6.72 (s, 1H, CH=), 6.83 (m, 2H, CH=), 6.93 (m, 2H, CH=). <sup>13</sup>C NMR (CDCl<sub>3</sub>): δ = 20.3 (CH<sub>3</sub>), 21.6 (CH<sub>3</sub>), 26.1 (CH<sub>3</sub>, NCH<sub>3</sub>), 46.2 (CH), 56.0 (CH<sub>3</sub>, OCH<sub>3</sub>), 107.6 (CH=), 109.7 (C), 111.1 (CH=), 122.0 (CH=), 122.2 (C), 122.8 (CH=), 123.6 (CH=), 124.2 (C), 127.5 (CH=), 138.1 (C), 144.1 (C), 157.3 (C), 177.8 (C=O). TOF-HRMS (ESI+): m/z = 284.1280, calcd. for C<sub>17</sub>H<sub>18</sub>NO<sub>3</sub> [M+H]<sup>+</sup>: 284.1287. ee determined by SFC using Chiralcel IC-3 column (flow: 3 ml/min, 85:15 scCO<sub>2</sub>:MeOH; λ = 210.0 nm). R<sub>T</sub> (major): 2.78 min, R<sub>T</sub> (minor): 3.17 min.

**3-(2',6'-Dimethylphenyl)-1-methylindolin-2-one 11:** Yield: 29.2 mg (93%) as a white solid (2% ee); <sup>1</sup>H NMR (CDCl<sub>3</sub>): δ = 1.64 (s, 3H, CH<sub>3</sub>), 2.58 (s, 3H, CH<sub>3</sub>), 3.32 (s, 3H, NCH<sub>3</sub>), 5.05 (s, 1H, CH), 6.90 (m, 3H, CH=), 6.97 (m, 1H, CH=), 7.12 (m, 2H, CH=), 7.30 (m, 1H, CH=). <sup>13</sup>C NMR (CDCl<sub>3</sub>): δ = 18.6 (CH<sub>3</sub>), 21.8 (CH<sub>3</sub>), 26.2 (CH<sub>3</sub>, NCH<sub>3</sub>), 48.1 (CH), 107.9 (CH=), 122.5 (CH=), 122.8 (CH=), 127.8 (CH=), 127.9 (CH=), 128.1 (CH=), 128.2 (CH=), 128.3 (C), 129.5 (CH=), 133.5 (C), 137.2 (C), 138.0 (C), 142.0 (C), 176.1 (C=O). TOF-HRMS (ESI+): m/z = 252.1385, calcd. for C<sub>17</sub>H<sub>19</sub>NO [M+H]<sup>+</sup>: 252.1388. ee determined by SFC using Chiralcel IC-3 column (flow: 3 ml/min, 90:10 scCO<sub>2</sub>:MeOH; λ = 254.0 nm). R<sub>T</sub> (major): 3.02 min, R<sub>T</sub> (minor): 4.31 min.

**1-Methyl-3-(2'-phenoxy-naphthalen-1-yl)indolin-2-one 12:** Yield: 33.2 mg (70%) as a yellowish solid ([α]<sub>D</sub><sup>20</sup>: +47.5° (c = 0.61 in CH<sub>2</sub>Cl<sub>2</sub>) for 28% ee); <sup>1</sup>H NMR (CDCl<sub>3</sub>): δ = 2.68 (s, 3H, NCH<sub>3</sub>), 4.80 (d, <sup>2</sup>J<sub>H-H</sub> = 11.4 Hz, 1H, CH<sub>2</sub>), 4.85 (d, <sup>2</sup>J<sub>H-H</sub> = 11.4 Hz, 1H, CH<sub>2</sub>), 5.29 (s, 1H, CH), 6.61 (d, <sup>3</sup>J<sub>H-H</sub> = 6.4 Hz, 1H, CH=), 6.92 (m, 4H, CH=), 7.27 (m, 6H, CH=), 7.43 (m, 1H, CH=), 7.61 (m, 1H, CH=), 7.85 (m, 1H, CH=), 8.15 (d, <sup>3</sup>J<sub>H-H</sub> = 6.8 Hz, 1H, CH=). <sup>13</sup>C NMR (CDCl<sub>3</sub>): δ = 25.6 (CH<sub>3</sub>, NCH<sub>3</sub>), 44.6 (CH), 70.7 (CH<sub>2</sub>), 107.8 (CH=), 114.1 (CH=), 118.9 (C), 121.9 (CH=), 122.3 (CH=), 123.2 (CH=), 123.6 (CH=), 127.3 (CH=), 127.9 (C), 128.3 (CH=), 128.5 (C), 128.6 (CH=), 128.8 (CH=), 129.4 (CH=), 129.5 (CH=), 129.6 (CH=), 134.1 (C), 136.2 (C), 144.6 (C), 153.8 (C), 177.1 (C=O). TOF-HRMS (ESI+): m/z = 380.1651, calcd. for C<sub>26</sub>H<sub>22</sub>NO<sub>2</sub> [M+H]<sup>+</sup>: 380.1638. ee determined by SFC using Chiralcel IC-3 column (flow: 3 ml/min, 70:30 scCO<sub>2</sub>:MeOH; λ = 254.0 nm). R<sub>T</sub> (+): 2.9 min (major), R<sub>T</sub> (-): 3.23 min (minor).

**3-(2'-Methoxynaphthalen-1-yl)-1-methylindolin-2-one 13:** Yield: 30.3 mg (80%) as a white solid ([α]<sub>D</sub><sup>20</sup>: +25.2° (c = 0.61 in CH<sub>2</sub>Cl<sub>2</sub>) for 15% ee); <sup>1</sup>H NMR (CDCl<sub>3</sub>): δ = 3.37 (s, 3H, NCH<sub>3</sub>), 3.61 (s, 3H, OCH<sub>3</sub>), 5.28 (s, 1H, CH), 6.90 (m, 3H, CH=), 7.21 (m, 2H, CH=), 7.42 (m, 1H, CH=), 7.58 (m, 1H, CH=), 7.85 (m, 2H, CH=), 8.15 (d, <sup>3</sup>J<sub>H-H</sub> = 7.0 Hz, 1H, CH=). <sup>13</sup>C NMR (CDCl<sub>3</sub>): δ = 26.6 (CH<sub>3</sub>, NCH<sub>3</sub>), 44.5 (CH), 57.2 (CH<sub>3</sub>), 107.5 (CH=), 114.6 (CH=), 122.1 (CH=), 122.4 (CH=), 122.6 (C), 122.8 (C), 123.4 (CH=), 122.3 (CH=), 123.7 (CH=), 126.9 (C), 127.7 (CH=), 128.6 (C), 129.6 (CH=), 130.1 (CH=), 133.9 (C), 154.7 (C), 177.0 (C=O). TOF-HRMS (ESI+): m/z = 303.1259, calcd. for C<sub>20</sub>H<sub>18</sub>NO<sub>2</sub> [M+H]<sup>+</sup>: 303.1265. ee determined by SFC using Chiralcel IC-3 column (flow: 3 ml/min, 90:10 scCO<sub>2</sub>:MeOH; λ = 254.0 nm). R<sub>T</sub> (+): 9.63 min (major), R<sub>T</sub> (-): 11.36 min (minor).

### Procedure for the kinetic experiments

In a flame-dried Schlenk tube, Pd<sub>2</sub>(dba)<sub>3</sub>·CHCl<sub>3</sub> (0.0019 mmol, 2.0 mg), phosphite-pyridine **L9c** (0.0049 mmol, 2.8 mg), substrate (25 mg, 0.0630 mmol), Meldrum's acid (2.5 eq, 0.1575 mmol, 22.7 mg) and hexamethylbenzene (1.7 mg, 0.0105) as internal standard were placed. Dry C<sub>6</sub>D<sub>6</sub> (3 mL) was added and 0.7 mL of this mixture were rapidly transferred to a NMR tube with a septum cap immediately before recording the NMR. Previously, the NMR tube was placed under vacuum and backfilled with N<sub>2</sub> (x3). The reaction was followed by recording the <sup>1</sup>H-NMR spectrum with a 1 min interval.

### Computational details

The geometries of all transition states were optimized employing B3LYP<sup>[26]</sup> functional including a D3 empirical dispersion correction as implemented in Gaussian 09 program.<sup>[27]</sup> LANL2DZ<sup>[28]</sup> basis set were used for palladium and the 6-31G\* basis set for all other elements.<sup>[29]</sup> Solvation correction was applied in the course of the optimizations using the PCM model with the default parameters for diethyl ether.<sup>[30]</sup> The energies were further refined by performing single-point calculations using the parameters mentioned before, with the exception that the 6-311+G\*\*<sup>[31]</sup> basis set was used for all elements except palladium. All energies reported are Gibbs free energies at 298.15 K and calculated as  $G_{\text{reported}} = G_{6-31G^*} + (E_{6-311+G^{**}} - E_{6-31G^*})$ .

### Acknowledgements

We gratefully acknowledge financial support from the Spanish Ministry of Economy and Competitiveness (CTQ2016-74878-P), European Regional Development Fund (AEI/FEDER, UE), the Catalan Government (2017SGR1472), and the ICREA Foundation (ICREA Academia award to M.D.). M. M. thanks MINECO for a fellowship. M.J. acknowledges the financial support for his PhD programme received from Molecular Medicine Ireland as part of the Clinical & Translational Research Scholars Programme (CTRSP), funded under the Programme for Research in Third Level Institutions (PRTL) Cycle 5, and co-funded under the European Regional Development Fund (ERDF).

### References

- [1] a) J. F. Hartwig, *Synlett* **2006**, 9, 1283-1294. b) D. A. Culkin, J. F. Hartwig, *Acc. Chem. Res.* **2003**, 36, 234-245. c) J. F. Hartwig, *Pure Appl. Chem.* **2009**, 71, 1417-1423. d) C. C. C. Johansson, T. J. Colacot, *Angew. Chem.* **2010**, 122, 686-718; *Angew. Chem. Int. Ed.* **2010**, 49, 676-707. e) S. T. Sivanandan, A. Shaji, I. Ibnuasaun, C. C. C. Johansson, T. J. Colacot, *Eur. J. Org. Chem.* **2015**, 1, 38-49.
- [2] a) Q.-Y. Shou, R.-Z. Fu, Q. Tan, Z.-W. Shen, *J. Agric. Food Chem.* **2009**, 57, 6712-6719. b) T. C. McKee, H. R. Bokesch, J. L. McCormick, M. A. Rashid, D. Spielvogel, K. R. Gustafson, M. M. Alavanja, J. H. Cardellina, M. R. Boyd, *J. Nat. Prod.* **1997**, 60, 431-438. c) M. Carril, R. SanMartin, F. Churruca, L. Tellitu, E. Dominguez, *Org. Lett.* **2005**, 7, 4787-4789. d) T. Honda, H. Namiki, F. Satoh, *Org. Lett.* **2001**, 3, 631-633. e) T. Honda, Y. Sakamaki, *Tetrahedron Lett.* **2005**, 46, 6823-6825.
- [3] a) S. R. S. Rudrangi, V. K. Bontha, V. R. Manda, S. Bethi, *Asian J. Research Chem.* **2011**, 4, 335-338. b) A. Jossang, P. Jossang, H. A. Hadi, T. Sevenet, B. Bodo, *J.*

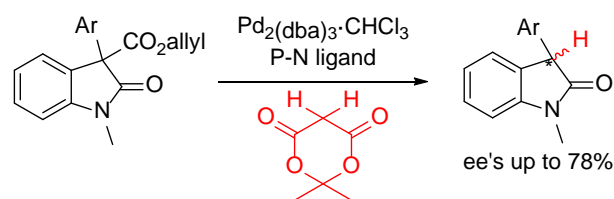
- Org. Chem.* **1991**, *56*, 6527-6530. c) K. Stratmann, R. E. Moore, R. Bonjouklian, J. B. Deeter, G. M. L. Patterson, S. Shaffer, C. D. Smith, T. A. Smitka, *J. Am. Chem. Soc.* **1994**, *116*, 9935-9942. d) Y.-Q. Tang, I. Sattler, R. Thiericke, S. Grabley, X.-Z. Feng, *Eur. J. Org. Chem.* **2001**, 261-267. e) T. Jiang, K. L. Kuhen, K. Wolff, H. Yin, K. Bieza, J. Caldwell, B. Bursulaya, T. Y.-H. Wu, Y. He, *Bioorg. Med. Chem. Lett.* **2006**, *16*, 2105-2108. f) T. Tokunaga, W. E. Hume, T. Umezome, K. Okazaki, Y. Ueki, K. Kumagai, S. Hourai, J. Nagamine, H. Seki, M. Taiji, H. Noguchi, R. Nagata, *J. Med. Chem.* **2001**, *44*, 4641-4649. g) H. Kitamura, A. Kato, T. Esaki, *Eur. J. Pharmacol.* **2001**, *418*, 225-227.
- [4] a) S. Lee, J. F. Hartwig, *J. Org. Chem.* **2001**, *66*, 3402-3415. Other examples for synthesis of chiral oxindoles via Pd-intramolecular cyclization reactions, see: b) Y.-X. Jia, J. M. Hillgre, E. L. Watson, S. P. Mardsen, E. P. Kündig, *Chem. Commun.* **2008**, 4040-4042 (ee's up to 90%). c) X. Luan, L. Xu, E. Drinkel, R. Mariz, F. Gatti, R. Dorta, *Org. Lett.* **2010**, *12*, 1912-1915 (ee's up to 94%). For Pd-intramolecular Heck reaction, see: d) A. B. Dounay, K. Hatanaka, J. K. Kodanko, M. Ostereich, L. E. Overman, L. A. Pfeifer, M. W. Weiss, *J. Am. Chem. Soc.* **2003**, *125*, 6261-6271 (ee's up to 98%).
- [5] For  $\alpha$ -arylation of ketones, see: a) D. A. Culkin, J. F. Hartwig, *Acc. Chem. Res.* **2003**, *36*, 234-245. b) M. Palucki, S. L. Buchwald, *J. Am. Chem. Soc.* **1997**, *119*, 11108-11109. c) T. Hamada, A. Chieffi, J. Ahman, S. L. Buchwald, *J. Am. Chem. Soc.* **2002**, *124*, 1261-1268. d) H. Muratake, M. Natsume, *Tetrahedron Lett.* **1997**, *38*, 7581-7582. For  $\alpha$ -arylation of esters, see: e) S. Lee, N. A. Beare, J. F. Hartwig, *J. Am. Chem. Soc.* **2001**, *123*, 8410-8411. f) W. A. Moradi, S. L. Buchwald, *J. Am. Chem. Soc.* **2001**, *123*, 7996-8002. g) E. Bentz, M. G. Moloney, S. M. Westaway, *Tetrahedron Lett.* **2004**, *45*, 7395-7397. For  $\alpha$ -arylation of nitriles, see: h) J. You, J. G. Verkade, *Angew. Chem.* **2003**, *115*, 5205-5207; *Angew. Chem., Int. Ed.* **2003**, *42*, 5051-5053. i) L. Wu, J. F. Hartwig, *J. Am. Chem. Soc.* **2005**, *127*, 15824-15832. For  $\alpha$ -arylation of amides, see: j) K. H. Shaughnessy, B. C. Hamann, J. F. Hartwig, *J. Org. Chem.* **1998**, *63*, 6546-6553. k) E. J. Hennessy, S. L. Buchwald, *J. Am. Chem. Soc.* **2003**, *125*, 12084-12085.
- [6] M. J. Durbin, M. C. Willis, *Org. Lett.* **2008**, *10*, 1413-1415.
- [7] a) R. A. Altman, A. M. Hyde, X. Huang, S. L. Buchwald, *J. Am. Chem. Soc.* **2008**, *130*, 9613-9620. b) P. Li, S. L. Buchwald, *Angew. Chem.* **2011**, *123*, 6520-6524; *Angew. Chem. Int. Ed.* **2011**, *50*, 6396-6400.
- [8] a) M. P. Carroll, H. Müller-Bunz, P. J. Guiry, *Chem. Commun.* **2012**, 48, 11142-11144. b) R. Doran, M. P. Carroll, R. Akula, B. F. Hogan, M. Martins, S. Fanning, P. J. Guiry, *Chem. Eur. J.* **2014**, *20*, 15354-15359. c) R. Doran, P. J. Guiry, *J. Org. Chem.* **2014**, *79*, 9112-9124. d) C. Kingston, P. J. Guiry, *J. Org. Chem.* **2017**, *82*, 3806-3813.
- [9] a) J. T. Mohr, T. Nishimata, D. C. Behenna, B. M. Stoltz, *J. Am. Chem. Soc.*, **2006**, *128*, 11348-11349. b) S. C. Marinescu, T. Nishimata, J. T. Mohr, B. M. Stoltz, *Org. Lett.* **2008**, *10*, 1039-1042. c) D. C. Behenna, B. M. Stoltz, in *Topics in Organometallic Chemistry* **2013**, *44*, 281-314.
- [10] a) R. Akula, R. Doran, P. J. Guiry, *Chem. Eur. J.* **2016**, *22*, 9938-9942. b) R. Akula, P. J. Guiry, *Org. Lett.* **2016**, *18*, 5472-5475. c) J. James, P. J. Guiry, *ACS Catal.* **2017**, *7*, 1397-1402.
- [11] M. Jackson, C. Q. O'Broin, H. Müller-Bunz, P. J. Guiry, *Org. Biomol. Chem.* **2017**, *15*, 8166-8178.
- [12] a) O. Pàmies, M. Diéguez, *Acc. Chem. Res.* **2010**, *43*, 312-322. b) P. W. N. M. van Leeuwen, P. C. J. Kamer, C. Claver, O. Pàmies, M. Diéguez, *Chem. Rev.* **2011**, *111*, 2077-2118. c) O. Pàmies, P. G. Andersson, M. Diéguez, *Chem. Eur. J.* **2010**, *16*, 14232-14240. d) M. Diéguez, O. Pàmies, *Isr. J. Chem.* **2012**, *52*, 572-581. e) O. Pàmies, M. Diéguez, *Chem. Rec.* **2016**, *16*, 2460-2481.
- [13] These ligands have been successfully applied to other metal-catalyzed asymmetric transformations. See: a) O. Pàmies, M. Diéguez, C. Claver, *J. Am. Chem. Soc.* **2005**, *127*, 3646-3647. b) M. Magre, M. Biosca, O. Pàmies, M. Diéguez, *ChemCatChem* **2015**, *7*, 114-120. c) R. Bellini, M. Magre, M. Biosca, M.; P.-O. Norrby, O. Pàmies, M. Diéguez, C. Moberg, *ACS Catal.* **2016**, *6*, 1701-1712. d) M. Diéguez, O. Pàmies, *Chem. Eur. J.* **2008**, *14*, 3653-3669. e) M. Diéguez, J. Mazuela, O. Pàmies, J. J. Verendel, P. G. Andersson, *Chem. Commun.* **2008**, 3888-3890. f) J. Mazuela, J. J. Verendel, M. Coll, B. Schäffner, A. Börner, P. G. Andersson, O. Pàmies, M. Diéguez, *J. Am. Chem. Soc.* **2009**, *131*, 12344-12353. g) J. Mazuela, O. Pàmies, M. Diéguez, *Chem. Eur. J.* **2010**, *16*, 3434-3440. h) J. Mazuela, O. Pàmies, M. Diéguez, *Chem. Eur. J.* **2013**, *19*, 2416-2432. i) J. Mazuela, O. Pàmies, M. Diéguez, *Adv. Synth. Catal.* **2013**, *355*, 2569-2583.
- [14] Disappointingly, the application of other successful ligands for Pd-decarboxylation reactions, such as the (*R,R*)-ANDEN-phenyl Trost and (*R,R*)-DACH-phenyl Trost ligands, provided the desired product in racemic form.
- [15] Similar behavior have been previously reported in the Pd-catalyzed decarboxylative protonation of  $\alpha$ -aryl- $\beta$ -keto allyl esters, for which the enantioselectivity also decreases for substrates lacking *ortho* methoxy substituents, see ref. 8a
- [16] On the other hand, based on experimental results, Guiry has proposed that in the key Pd-enolate intermediate using ligand **1**, the preferential attack of the proton electrophile through one of the enolate faces is controlled by both the oxazoline substituent and the presence of the *ortho*-substituents in the aryl group, see ref. 8a
- [17] This behavior is similar to that observed in enantioselective allylation, see: J. A. Keith, D. C. Behenna, J. T. Mohr, S. Ma, S. C. Marinescu, J. Oxgaard, B. M. Stoltz, W. A. Goddard III, *J. Am. Chem. Soc.* **2007**, *129*, 11876-11877.

- [18] A priori based on the catalytic results, this seems the most likely catalytic pathway since the best enantioselectivities are achieved with the pyridine-based ligands.
- [19] E. M. Simmons, J. F. Hartwig, *Angew. Chem.* **2012**, *124*, 3120-3126; *Angew. Chem. Int. Ed.* **2012**, *51*, 3066-3072.
- [20] C. Johansson, G. C. Lloyd-Jones, P.-O. Norrby, *Tetrahedron: Asymmetry* **2010**, *21*, 1585-1592.
- [21] Protonation through the enol tautomer of Meldrum's acid has been excluded, because it exists predominantly in the diketo tautomer form (>99.5%), see: H. McNab, *Chem. Soc. Rev.* **1978**, *7*, 345-358.
- [22] In these DFT calculations (including those using substrates **S4** and **S6**, see below), the magnitude of the enantioselectivity is overestimated by the calculations, albeit the general trend is reproduced well. Therefore the calculated ee decreased upon removal of the *ortho* methoxy groups of the substrate as observed experimentally. The overestimation of the calculated ee could most likely indicate an error in the close contact energies when using our chosen DFT method in conjunction with a continuum solvation model.
- [23] S. S. Zaleskiy, V. P. Ananikov, *Organometallics*, **2012**, *31*, 2302-2309.
- [24] C. A. Citron, P. Rabe, L. Barra, C. Nakano, T. Hoshino, J. S. Dickschat, *Eur. J. Org. Chem.*, **2014**, 7684-7691.
- [25] G. J. H. Buisman, P. C. J. Kamer, P. W. N. M. van Leeuwen, *Tetrahedron: Asymmetry* **1993**, *4*, 1625-1634.
- [26] a) C. Lee, W. Yang, R. G. Parr, *Phys. Rev. B* **1988**, *37*, 785-789. b) A. D. Becke, *J. Chem. Phys.* **1993**, *98*, 5648-5652.
- [27] M. J. Frisch, G. W. Trucks, H. B. Schlegel, G. E. Scuseria, M. A. Robb, J. R. Cheeseman, G. Scalmani, V. Barone, B. Mennucci, G. A. Petersson, H. Nakatsuji, M. Caricato, X. Li, H. P. Hratchian, A. F. Izmaylov, J. Bloino, G. Zheng, J. L. Sonnenberg, M. Hada, M. Ehara, K. Toyota, R. Fukuda, J. Hasegawa, M. Ishida, T. Nakajima, Y. Honda, O. Kitao, H. Nakai, T. Vreven, J. A. Montgomery, J. E. Peralta Jr., F. Ogliaro, M. Bearpark, J. J. Heyd, E. Brothers, K. N. Kudin, V. N. Staroverov, R. Kobayashi, J. Normand, K. Raghavachari, A. Rendell, J. C. Burant, S. S. Iyengar, J. Tomasi, M. Cossi, N. Rega, J. M. Millam, M. Klene, J. E. Knox, J. B. Cross, V. Bakken, C. Adamo, J. Jaramillo, R. Gomperts, R. E. Stratmann, O. Yazyev, A. J. Austin, R. Cammi, C. Pomelli, J. W. Ochterski, R. L. Martin, K. Morokuma, V. G. Zakrzewski, G. A. Voth, P. Salvador, J. J. Dannenberg, S. Dapprich, A. D. Daniels, O. Farkas, J. B. Foresman, J. V. Ortiz, J. Cioslowski, D. J. Fox, Revision A.02 ed; Gaussian: Wallingford, CT, 2009.
- [28] P. J. Hay, W. R. Wadt, *J. Chem. Phys.* **1985**, *82*, 299-310.
- [29] a) W. J. Hehre, R. Ditchfield, J. A. Pople, *J. Chem. Phys.* **1972**, *56*, 2257-2261. b) P. C. Hariharan, J. A. Pople, *Theor. Chim. Acta* **1973**, *28*, 213-222. c) M. M. Francl, W. J. Pietro, W. J. Hehre, J. S. Binkley, M. S. Gordon, D. J. Defrees, J. A. Pople, *J. Chem. Phys.* **1982**, *77*, 3654-3665.
- [30] a) S. Miertus, J. Tomasi, *Chem. Phys.* **1982**, *65*, 239-245. b) B. Mennucci, J. Tomasi, *J. Chem. Phys.* **1997**, *106*, 5151-5158. c) M. Cossi, V. Barone, B. Mennucci, J. Tomasi, *Chem. Phys. Lett.* **1998**, *286*, 253-260.
- [31] a) R. Krishnan, J. S. Binkley, R. Seeger, J. A. Pople, *J. Chem. Phys.* **1980**, *72*, 650-654. b) A. D. McLean, G. S. Chandler, G. S. *J. Chem. Phys.* **1980**, *72*, 5639-5648.

Enantioselective Synthesis of Sterically Hindered Tertiary  $\alpha$ -Aryl Oxindoles via Pd-Catalyzed Decarboxylative Protonation. An Experimental and Theoretical Mechanistic Investigation

*Adv. Synth. Catal.* **Year**, *Volume*, Page – Page

Maria Biosca, Mark Jackson, Marc Magre, Oscar Pàmies,\* Per-Ola Norrby,\* Montserrat Diéguez,\* and Patrick J. Guiry\*



Protonation as stereodetermining step  
Decarboxylation as rate-determining step